

Rowan University

Rowan Digital Works

School of Osteopathic Medicine Faculty
Scholarship

School of Osteopathic Medicine

5-1-2009

The PKC Inhibitor Ro31-8220 Blocks Acute Amphetamine-Induced Dopamine Overflow in the Nucleus Accumbens

Jessica Loweth

Rowan University School of Osteopathic Medicine

Robyn Svoboda

University of Chicago

Jennifer Austin

University of Chicago

Anitra Guillory

University of Chicago

Paul Vezina

University of Chicago

Follow this and additional works at: https://rdw.rowan.edu/som_facpub



Part of the [Biochemistry Commons](#), [Biology Commons](#), [Chemicals and Drugs Commons](#), [Endocrinology Commons](#), [Neuroscience and Neurobiology Commons](#), [Pharmacology Commons](#), and the [Substance Abuse and Addiction Commons](#)

Recommended Citation

Loweth JA, Svoboda R, Austin JD, Guillory AM, Vezina P. The PKC inhibitor Ro31-8220 blocks acute amphetamine-induced dopamine overflow in the nucleus accumbens. *Neuroscience Letters*. 2009 May 15;455(2):88-92. Epub 2009 Mar 11. doi: 10.1016/j.neulet.2009.03.012. PMID: 19368852. PMCID: PMC2688659.

This Article is brought to you for free and open access by the School of Osteopathic Medicine at Rowan Digital Works. It has been accepted for inclusion in School of Osteopathic Medicine Faculty Scholarship by an authorized administrator of Rowan Digital Works.

Published in final edited form as:

Neurosci Lett. 2009 May 15; 455(2): 88–92. doi:10.1016/j.neulet.2009.03.012.

The PKC Inhibitor Ro31-8220 Blocks Acute Amphetamine-Induced Dopamine Overflow in the Nucleus Accumbens

Jessica A. Loweth^{1,*}, Robyn Svoboda², Jennifer D. Austin², Anitra M. Guillory¹, and Paul Vezina^{1,2}

¹ Committee on Neurobiology, The University of Chicago, Chicago, IL

² Department of Psychiatry and Behavioral Neuroscience, The University of Chicago, Chicago, IL

Abstract

Acute administration of the psychostimulant amphetamine increases extracellular levels of dopamine (DA) by reversing the DA transporter on ascending midbrain DA neurons. *In vitro* studies using striatal synaptosomal, slice and nucleus accumbens (NAcc) tissue preparations have implicated protein kinase C (PKC) in this effect. The present study further examined this effect *in vivo* by assessing the ability of the PKC inhibitor, Ro31-8220 (10 μ M), to inhibit acute amphetamine-induced DA overflow when applied with this drug to the NAcc via reverse dialysis. Amphetamine was applied at a concentration of 30 μ M and the core and shell subregions of the NAcc were assayed separately in freely moving rats. These brain regions play a role in the acute locomotor-activating and motivational effects of amphetamine. Consistent with the findings of previous *in vitro* experiments, reverse dialysis of Ro31-8220 with amphetamine robustly attenuated the ability of this drug to increase extracellular levels of dopamine in both the core and shell subregions of the NAcc. These results confirm that amphetamine stimulates dopamine overflow via a PKC-dependent mechanism.

Keywords

dopamine overflow; nucleus accumbens; PKC; amphetamine; microdialysis

Psychomotor stimulant drugs like amphetamine (AMPH) increase locomotion and support self-administration [29,30,31]. There is wide-spread acceptance that AMPH produces these effects through an action-potential independent mechanism by interacting with the dopamine transporter (DAT) to increase extracellular levels of dopamine (DA) in the nucleus accumbens (NAcc), the major subcortical projection field of midbrain DA neurons [18,21,26]. The outward-facing, membrane-bound form of DAT can bind AMPH, transport the drug into the nerve terminal, release the AMPH in exchange for DA, and transport the neurotransmitter out of the neuron, releasing it into the extracellular space [5,15,26]. In addition to this exchange diffusion mechanism, a number of studies have demonstrated that additional intracellular signal transduction mechanisms may also play a role in AMPH-induced DA release.

There is evidence that the cytoplasmic serine/threonine protein kinase C (PKC) contributes importantly to AMPH-stimulated DA release. The PKC activator phorbol ester 12-*o*-

*, Correspondence: Jessica Loweth, 5841 South Maryland Avenue, MC 3077, Chicago, IL 60637, TEL: (773) 702-2891, FAX: (773) 702-0857, E-MAIL: E-mail: jloweth@uchicago.edu.

Publisher's Disclaimer: This is a PDF file of an unedited manuscript that has been accepted for publication. As a service to our customers we are providing this early version of the manuscript. The manuscript will undergo copyediting, typesetting, and review of the resulting proof before it is published in its final citable form. Please note that during the production process errors may be discovered which could affect the content, and all legal disclaimers that apply to the journal pertain.

tetradecanoyl phorbol-13-acetate (TPA) mimics the effect of AMPH by producing an increase in DA release in striatal slices and synaptosomes, an effect blocked by the DAT antagonists cocaine and GBR 12935 [3]. Conversely, the PKC inhibitor Ro31-8220 blocks Ca^{2+} -independent AMPH-induced DA release in rat striatal slices [16]. In addition, perfusion of NAcc tissue with Ro31-8220 blocks AMPH-stimulated DA release and, when infused into the NAcc, attenuates locomotor responding to intra-accumbens AMPH [1].

Together, the above findings indicate that PKC activity contributes to AMPH-stimulated DA release in the striatum and NAcc *in vitro*. These findings also suggest that inhibiting NAcc PKC activity *in vivo* attenuates locomotor responding to NAcc AMPH, presumably by preventing AMPH-stimulated DA release in this region [18,29]. The present experiments assessed this possibility by investigating whether reverse dialysis of the selective PKC inhibitor Ro31-8220 with AMPH attenuates the ability of this drug to increase extracellular levels of DA in the NAcc in freely moving rats. The core and shell subregions of the NAcc were investigated as both are known to contribute to the behavioral effects of AMPH [27].

Male Sprague-Dawley rats (Harlan Sprague-Dawley, Madison, WI) weighing 250–275 g upon arrival were used. They were individually housed in a 12 h light/12 h dark reverse cycle room with food and water freely available at all times. All experiments were conducted in accordance with the Declaration of Helsinki and the Guide for the Care and Use of Laboratory animals as promulgated by the National Institutes of Health. All surgical procedures were conducted according to an approved Institutional Animal Care and Use Committee protocol.

Starting 3–5 days after arrival, rats were surgically implanted with chronic indwelling cannulae aimed at the NAcc core or shell. Rats were anesthetized with a ketamine-xylazine mixture (100 mg/kg-6 mg/kg, i.p.), placed in a stereotaxic instrument with the incisor bar 5.0 mm above the interaural line, and implanted intracranially with bilateral guide cannulae (20 gauge, Plastics One, Roanoke, VA) aimed at the NAcc core (A/P +3.4 mm, M/L \pm 1.5 mm, D/V –6.5 to –8.5 mm) or NAcc shell (A/P +3.4 mm, M/L \pm 0.8 mm, D/V –6.5 to –8.5 mm). D/V coordinates are expressed from skull surface to the active length of the subsequently inserted microdialysis probe. Guide cannulae were angled at 10° to the vertical, positioned 5 mm above the ventral-most aspect of the NAcc [25], and anchored in place with dental cement fixed to stainless steel screws. Following surgery obturators were inserted into the guide cannulae and rats were returned to their home cages for a 7–10 day recovery period.

In vivo microdialysis was performed in eight Plexiglass chambers (38 × 32 × 34 cm) with stainless steel wire floors that were housed inside light- and sound-attenuating ventilated boxes. On the day before testing, rats were anesthetized briefly with isoflurane and a microdialysis probe was lowered into the NAcc core or shell. Concentric probes were constructed as described previously [14] with a 2 mm active surface length and a 5000 MW cutoff. Rats were placed individually in a testing chamber overnight where they were connected via a steel spring tether to a liquid swivel and collection vial positioned outside the chamber. Although tethered during testing, freely moving rats had free access to the entire chamber. Probes were perfused with aCSF (145 mM Na^+ , 2.7 mM K^+ , 1.2 mM Ca^{2+} , 1.0 mM Mg^{2+} , 150 mM Cl^- , pH=7.4) at a flow rate of 0.3 μ l/min overnight and 1.5 μ l/min during testing. To maximize data collection, rats were tested on two occasions, once on each side. Because no drugs were administered systemically during testing, n/group is expressed as probes used (experiments conducted) per condition.

Samples were collected every 20 minutes for a total of four hours of testing. Three baseline samples were first collected. One hour into the test session, the PKC inhibitor Ro31-8220 (0, 10 or 100 μ M) was added to the aCSF and perfused into the NAcc for the next two hours. Two hours into the test session, AMPH (0 or 30 μ M) was added to the PKC inhibitor and perfused

into the NAcc for one hour. Three hours into the test session and for the final hour of testing, the PKC inhibitor and the AMPH were removed from the aCSF. In this way, four treatment conditions were tested: AMPH alone, AMPH + Ro31-8220, Ro31-8220 alone, and aCSF. Ro31-8220 methanesulfonate salt and D-AMPH sulfate (Sigma Aldrich, St. Louis, MO) were dissolved freshly in aCSF either in combination or alone.

Dialysate samples (30 μ l) were stored at -80° C until analyzed for DA using HPLC with electrochemical detection (EC). HPLC-EC was conducted using a single-piston Gilson 302 pump (Gilson, Middleton, WI) set to 1.1 ml/min, a Gilson diaphragm type pulse dampener, a 10 cm ODS-C18 3 mm column (maintained at 35° C), an ESA Model 5100 Coulochem detector with a conditioning cell (oxidizing at +300 mV) placed prior to a Model 5011 high sensitivity analytical cell (electrodes set to +50 mV and -350 mV) and a 0.04 M sodium acetate mobile phase containing 0.3 mM Na_2 EDTA, 0.5 mM octyl sodium sulfate and 3.3% acetonitrile (pH 3.75). 25 μ l samples were introduced into the mobile phase via a Rheodyne injection valve. Extracellular concentrations of DA were estimated from peak areas using EZChrom Elite software. DA eluted at 4.8 min. To control for differences in active surface lengths between probes, DA concentrations were corrected for individual probe recoveries. These were determined *in vitro* at 20° C after each microdialysis testing session and ranged from 5 to 9%.

At the conclusion of the experiment, rats were anesthetized with sodium pentobarbital and perfused via intracardiac infusion of saline and 10% formalin. Brains were removed and postfixed in 10% formalin. Coronal sections (40 μ m) were mounted onto gelatin-coated slides and stained with cresyl violet for verification of probe placements. Only subjects with probes with active surface lengths in the NAcc core or shell were included in the data analyses (Figure 1). Twelve rats were excluded for failing to meet this criterion [AMPH, 2; AMPH + Ro31-8220 (10 μ M), 3; Ro31-8220 (10 μ M), 1; Ro31-8220 (100 μ M), 4; aCSF, 2]. Data were analyzed with one-way ANOVA followed by post-hoc LSD test comparisons according to Kirk [20]. ANOVA are resistant to violation of the homogeneity of variance assumption. However, the finding that this assumption was violated and that n/group were unequal required that the data be subjected to a transformation. The square root transformation was therefore applied to all the data and the resulting numbers analyzed with one-way ANOVA.

The effects of the different concentrations of Ro31-8220 alone on extracellular DA concentrations in the NAcc core and shell were first assessed. As shown in Table 1, the highest concentration of Ro31-8220 (100 μ M) by itself significantly increased extracellular concentrations of DA in both NAcc subregions ($p < 0.01$), indicating that at this concentration Ro31-8220 produces non-specific effects that precluded further testing. The lower concentration of Ro31-8220 tested (10 μ M) was without significant effects and so was used in all subsequent experiments.

As illustrated in Figure 2 (NAcc core) and Figure 3 (NAcc shell), 10 μ M Ro31-8220 significantly attenuated the ability of AMPH to increase extracellular levels of DA in both subregions of the NAcc when co-infused with the drug into these sites. No significant group differences were detected in NAcc DA overflow in either site in the first (aCSF) or second (Ro31-8220 alone) hours of testing. As expected, extracellular levels of NAcc DA increased precipitously upon the introduction of AMPH in the third hour of testing, but this increase was significantly dampened when AMPH was administered with Ro31-8220. One-way ANOVAs conducted on the maximal DA overflow observed for each animal during this period revealed a significant effect of groups in both the NAcc core ($F_{3,19} = 11.56$, $p < 0.001$) and NAcc shell ($F_{3,22} = 14.68$, $p < 0.001$). In the NAcc core, post-hoc LSD tests showed that the AMPH-induced DA overflow observed in the AMPH+Ro condition was significantly lower than in the AMPH alone condition ($p < 0.01$, Figure 2 inset) but remained significantly higher than that observed with Ro31-8220 and aCSF alone ($p < 0.05$). Similar effects were observed in the NAcc shell

(Figure 3 inset). In this case, the AMPH-induced DA overflow observed with AMPH+Ro was significantly lower than with AMPH alone ($p < 0.05$) but remained significantly higher than that observed with Ro31-8220 and aCSF alone ($p < 0.01$). Upon removal of the AMPH and Ro31-8220 in the fourth hour of testing, extracellular levels of NAcc DA returned rapidly to those maintained throughout testing by aCSF alone.

The present results show that *in vivo* reverse dialysis of the PKC inhibitor Ro31-8220 in either the NAcc core or shell attenuates the ability of AMPH to increase extracellular levels of DA in these regions. This finding is consistent with previous reports showing that Ro31-8220 inhibits AMPH-stimulated DA release in the NAcc and striatum *in vitro* [1,16] and extends others showing that NAcc Ro31-8220 attenuates the locomotor response of AMPH in this site [1], a behavior associated with this drug's ability to increase extracellular levels of NAcc DA [17,18]. Taken together, these findings suggest that PKC influences behavioral responding to AMPH by regulating DA overflow in the NAcc core and shell.

In contrast to the present findings, a previous study reported that reverse dialysis of the PKC inhibitor bisindolylmaleimide I (BIM, 30 μ M) into the rat striatum did not alter DA release in response to systemically administered AMPH (5 mg/kg, i.p.) [23]. These findings are difficult to reconcile. It should be noted however that co-infusion of Ro31-8220 with AMPH into the NAcc in the present study permitted assessment of the effects of PKC inhibition directly at the site of AMPH-induced overflow. This was not confounded by the effects AMPH would be expected to exert, when administered systemically, in sites adjacent to the microdialysis probe potentially not affected by the PKC inhibition. Additional differences between the two experiments that may have contributed to the different findings obtained include the different PKC inhibitors tested and the different brain regions assessed.

Although Ro31-8220 would also be expected to influence PKC activity in non-DA cells in the NAcc, it is unlikely that these actions could explain its ability to inhibit AMPH-induced NAcc DA overflow because the latter is Ca^{2+} -independent. Rather, several lines of evidence suggest that Ro31-8220 produces this effect by altering AMPH-induced reverse transport of DA through the DAT without affecting AMPH or DA uptake into the DA terminal [1]. There are known consensus sequences for PKC on the DAT [6] and deleting a region of DAT thought to include such PKC substrate sites abolishes AMPH-induced DA efflux from DAT expressing HEK-293 cells [19]. Moreover, the β_I and β_{II} isoforms of PKC co-immunoprecipitate with DAT and overexpressing PKC β_{II} enhances AMPH-stimulated DA efflux again from DAT expressing HEK-293 cells [13]. In addition, AMPH increases particulate PKC activity [7,8] and leads to increased PKC phosphorylation of (S41) neuromodulin, the calmodulin-binding protein thought to modulate transmitter release [10,11]. Although AMPH activates PKC and results in PKC-dependent phosphorylation, it is not known whether PKC produces its effects by directly phosphorylating DAT or other DAT-associated proteins [6]. Interestingly, PKC isoforms also interact with proteins that bind to DAT, such as the receptor for activated C kinases (RACK1) [22] and the PKC α -binding protein PICK 1 [28]. Taken together, these results suggest that PKC activity contributes to AMPH-mediated DA overflow by interacting with the DAT to promote DA efflux. This contribution of PKC was observed in both the NAcc core and shell even though DAT density is known to be higher in the core relative to the shell [32] and greater AMPH-induced DA overflow was observed in the former compared to the latter subregion in the present experiments.

PKC may also enhance AMPH-mediated DA efflux by altering DAT trafficking. AMPH is known to regulate DAT trafficking. For example, incubation of striatal synaptosomes with AMPH for short time periods (0.5–1.0 min) increases DAT surface expression [12], while longer exposure to AMPH leads to DAT internalization [9,33]. Similarly, persistent activation of PKC increases DAT endocytosis and decreases DAT surface expression [4,33]. Indeed, it

was recently shown that PKC β knockout mice show a reduction in DAT surface levels and altered AMPH-induced DAT trafficking as well as reduced AMPH-stimulated DA efflux compared to wild-type mice [2]. Thus, it is conceivable that Ro31-8220 inhibited AMPH-induced DA overflow in the present experiments by preventing the trafficking of DAT to the membrane. Whatever the case, the present findings clearly demonstrate an important role for PKC activity in acute AMPH-induced DA overflow in both the NAcc core and shell.

Acknowledgments

This study was supported by National Institutes of Health grants DA-09397 (P.V.), T32-DA-07255 (A.M.G.) and F31-DA-022834 (J.A.L.).

References

1. Browman KE, Kantor L, Richardson S, Badiani A, Robinson TE, Gnegy ME. Injection of the protein kinase C inhibitor Ro31-8220 into the nucleus accumbens attenuates the acute response to amphetamine: tissue and behavioral studies. *Brain Research* 1998;814:112–119. [PubMed: 9838071]
2. Chen R, Furman CA, Zhang M, Kim MN, Gereau RW IV, Leitges M, Gnegy ME. Protein kinase C β is a critical regulator of dopamine transporter trafficking and regulates the behavioral response to amphetamine in mice. *J Pharm Exp Ther* 2008;#147959.10.1124/jpet.108.147959EPub-IN PRESS
3. Cowell RM, Kantor L, Keikilani Hewlett GH, Frey KA, Gnegy ME. Dopamine transporter antagonists block phorbol ester-induced dopamine release and dopamine transporter phosphorylation in striatal synaptosomes. *Eur J Pharmacol* 2000;389:59–65. [PubMed: 10686296]
4. Daniels GM, Amara SG. Regulated trafficking of the human dopamine transporter. Clathrin-mediated internalization and lysosomal degradation in response to phorbol esters. *J Biol Chem* 1999;35794–35801. [PubMed: 10585462]
5. Fischer JF, Cho AK. Chemical release of dopamine from striatal homogenates: Evidence for an exchange diffusion model. *J Pharm Exp Ther* 1979;208:203–209.
6. Foster JD, Pananusorn B, Vaughan RA. Dopamine transporters are phosphorylated on N-terminal serines in rat striatum. *J Biol Chem* 2002;277:25178–25186. [PubMed: 11994276]
7. Giambalvo CT. Protein kinase C and dopamine transport—2. Effects of amphetamine in vitro. *Neuropharmacology* 1992;31:1211–1222. [PubMed: 1361666]
8. Gnegy ME. The effect of phosphorylation on amphetamine-mediated outward transport. *European Journal of Pharmacology* 2003;479:83–91. [PubMed: 14612140]
9. Gulley JM, Doolen S, Zahniser NR. Brief, repeated exposure to substrates down-regulates dopamine transporter function in *Xenopus* oocytes in vitro and rat dorsal striatum in vivo. *J Neurochem* 2002;83:400–411. [PubMed: 12423250]
10. Iwata S, Hewlett GHK, Ferrell ST, Czernik AJ, Meiri KF, Gnegy ME. Increased in vivo phosphorylation state of neuromodulin and synapsin I in striatum from rats treated with repeated amphetamine. *J Pharm Exp Ther* 1996;278:1428–1434.
11. Iwata S, Hewlett GHK, Gnegy ME. Amphetamine increases the phosphorylation of neuromodulin and synapsin I in rat striatal synaptosomes. *Synapse* 1997;26:281–291. [PubMed: 9183817]
12. Johnson LA, Furman CA, Zhang M, Guptaroy B, Gnegy ME. Rapid delivery of the dopamine transporter to the plasmalemmal membrane upon amphetamine stimulation. *Neuropharmacology* 2005;49:750–758. [PubMed: 16212991]
13. Johnson LA, Guptaroy B, Lund D, Shamban S, Gnegy ME. Regulation of amphetamine-stimulated dopamine efflux by protein kinase C β . *J Biol Chem* 2005;280:10914–10919. [PubMed: 15647254]
14. Jolly D, Vezina P. In vivo microdialysis in the rat: low cost and low labor construction of a small diameter, removable, concentric style microdialysis probe system. *J Neurosci Methods* 1996;68:259–267. [PubMed: 8912199]
15. Kahlig KM, Galli A. Regulation of dopamine transporter function and plasma membrane expression by dopamine, amphetamine, and cocaine. *Eur J of Pharm* 2003;479:153–158.
16. Kantor L, Gnegy ME. Protein kinase C inhibitors block amphetamine-mediated dopamine release in rat striatal slices. *J Pharm Exp Ther* 1998;284:592–598.

17. Kelly PH, Moore KE. Mesolimbic dopaminergic neurons in the rotational model of nigrostriatal function. *Nature* 1976;263:695–696. [PubMed: 980114]
18. Kelly PH, Seviour PW, Iversen SD. Amphetamine and apomorphine responses in the rat following 6-OHDA lesions of the nucleus accumbens septi and corpus striatum. *Brain Res* 1975;94:507–522. [PubMed: 1171714]
19. Khoshbouei H, Sen N, Guptaroy B, Johnson LA, Lund D, Gnegy ME, Galli A, Javitch JA. N-terminal phosphorylation of the dopamine transporter is required for amphetamine-induced efflux. *PLoS Biol* 2004;2(3):0387–0393.
20. Kirk, RE. Experimental design: procedures for the behavioral sciences. Brooks/Cole; Pacific Grove, CA: 1968.
21. Kuczenki, R.; Segal, DS. Neurochemistry of amphetamine. In: Cho, AK.; Segal, DS., editors. AMPH and its analogs: psychopharmacology, toxicology and abuse. Academic Press; San Diego: 1994. p. 81-113.
22. Lee KH, Kim MY, Kim DH, Lee YS. Syntaxin 1A and receptor for activated C kinase interact with the N-terminal region of human dopamine transporter. *Neurochem Res* 2004;29:1405–1409. [PubMed: 15202772]
23. Nair SG, Gudelsky GA. Protein kinase C inhibition differentially affects 3,4 – methylenedioxymethamphetamine-induced dopamine release in the striatum and prefrontal cortex of the rat. *Brain Research* 2004;1013:168–173. [PubMed: 15193525]
24. Paxinos, G.; Watson, C. The rat brain in stereotaxic coordinates, compact. Vol. 3. Academic Press; San Diego, CA: 1997.
25. Pellegrino, LJ.; Pellegrino, AS.; Cushman, AJ. A Stereotaxic Atlas of the Rat Brain. Plenum Press; New York: 1979.
26. Seiden LS, Sabol KE, Ricaurte GA. Amphetamine: effects on catecholamine systems and behavior. *Annu Rev Pharmacol Toxicol* 1993;33:639–677. [PubMed: 8494354]
27. Sellings LHL, Clarke PBS. Segregation of amphetamine reward and locomotor stimulation between nucleus accumbens medial shell and core. *J Neurosci* 2003;23:6295–6303. [PubMed: 12867514]
28. Torres GE, Yao WD, Mohn AR, Quan H, Kim KM, Levy AI, Staudinger J, Caron MG. Functional interaction between monoamine plasma membrane transporters and the synaptic PDZ domain-containing protein PICK1. *Neuron* 2001;30:121–134. [PubMed: 11343649]
29. Vezina P. Sensitization of midbrain dopamine neuron reactivity and the self-administration of psychomotor stimulant drugs. *Neurosci Biobehav Rev* 2004;27:827–839. [PubMed: 15019432]
30. Vezina P, Lorrain DS, Arnold GA, Austin JD, Suto N. Sensitization of midbrain dopamine neuron reactivity promotes the pursuit of amphetamine. *J Neurosci* 2002;22:4654–4662. [PubMed: 12040071]
31. Vezina P, Pierre PJ, Lorrain DS. The effect of previous exposure to amphetamine on drug-induced locomotion and self-administration of a low dose of the drug. *Psychopharmacology* 1999;147:125–134. [PubMed: 10591879]
32. Zahm DS. Functional-anatomical implications of the nucleus accumbens core and shell subterritories. *Annals New York Academy of Sciences* 1999;877:113–128.
33. Zahniser NR, Sorkin A. Rapid regulation of the dopamine transporter: role in stimulant addiction? *Neuropharmacology* 2004;47(Suppl 1):1979–1986.

NAcc Core

NAcc Shell

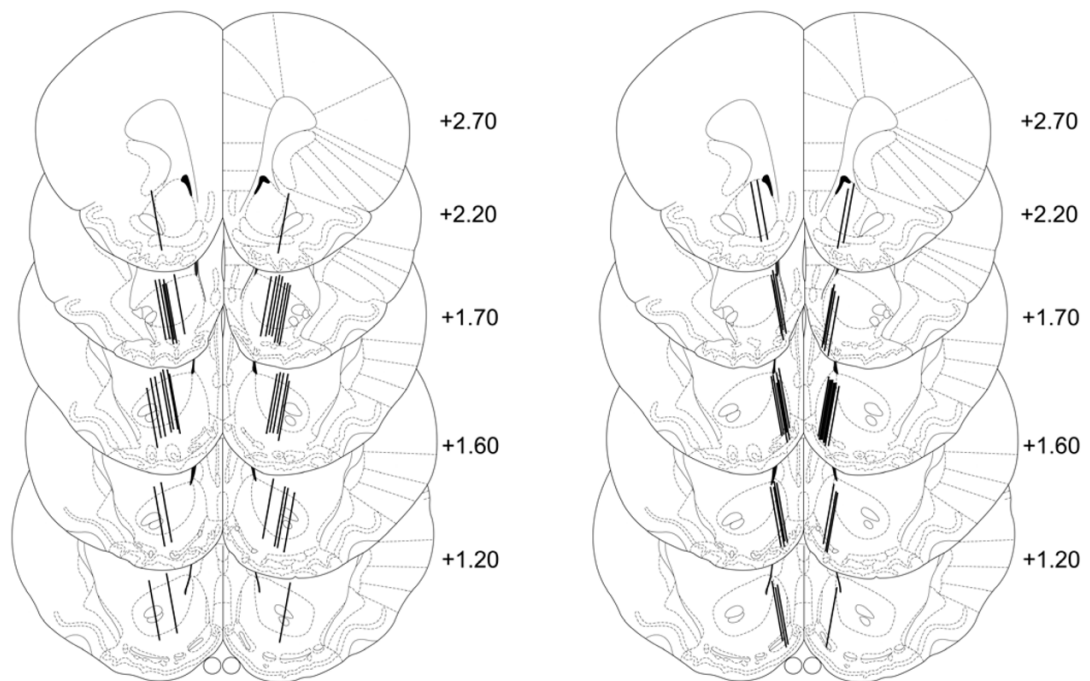


Figure 1. Location of the active portion of the microdialysis probes in the NAcc core (LEFT) and shell (RIGHT)

Line drawings are from the atlas of Paxinos and Watson [24]. Numbers to the right indicate mm from bregma. 36 experiments (18 experiments/side) were conducted in the NAcc core and 38 (19 experiments/side) in the NAcc shell.

NAcc Core

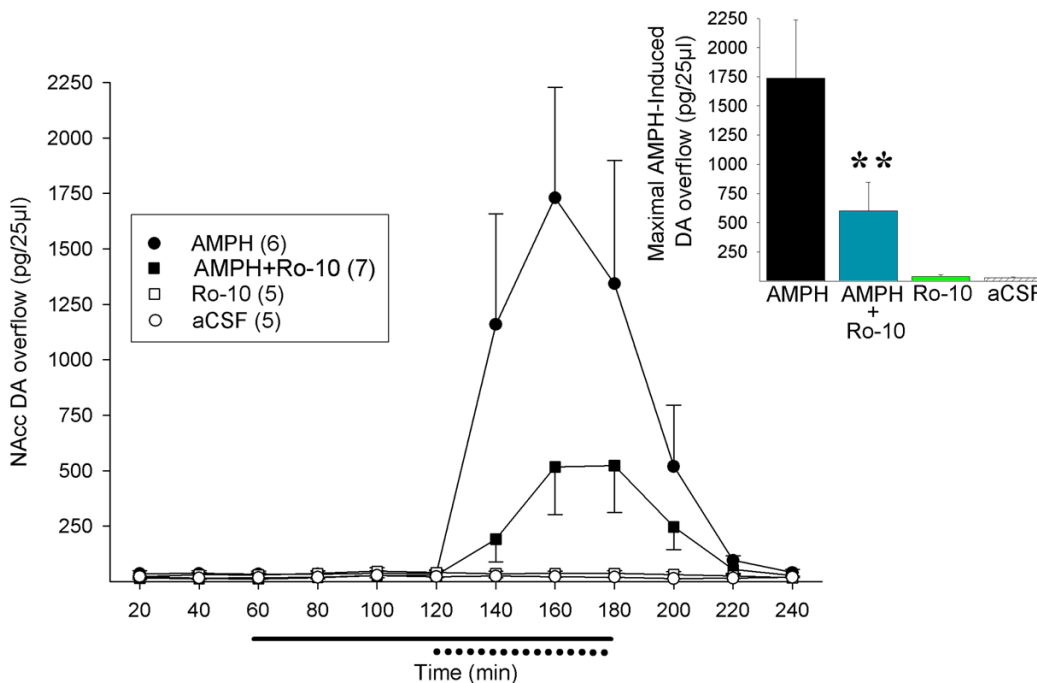


Figure 2. The PKC inhibitor Ro31-8220 attenuates the ability of AMPH to increase extracellular DA in the NAcc core
 Data are shown as group mean (\pm SEM) extracellular concentrations of DA in the NAcc core before, during and after reverse dialysis of Ro31-8220 (0 or 10 μ M, solid line at abscissa) and AMPH (0 or 30 μ M, dotted line at abscissa). **Inset.** Results are summarized as group mean (\pm SEM) maximal NAcc DA overflow induced by AMPH. Maximal overflow for each animal was taken as the highest DA peak obtained during reverse dialysis of AMPH. **, $p < 0.01$, AMPH vs. AMPH + Ro31-8220. Numbers in the legend indicate experiments/group.

NAcc Shell

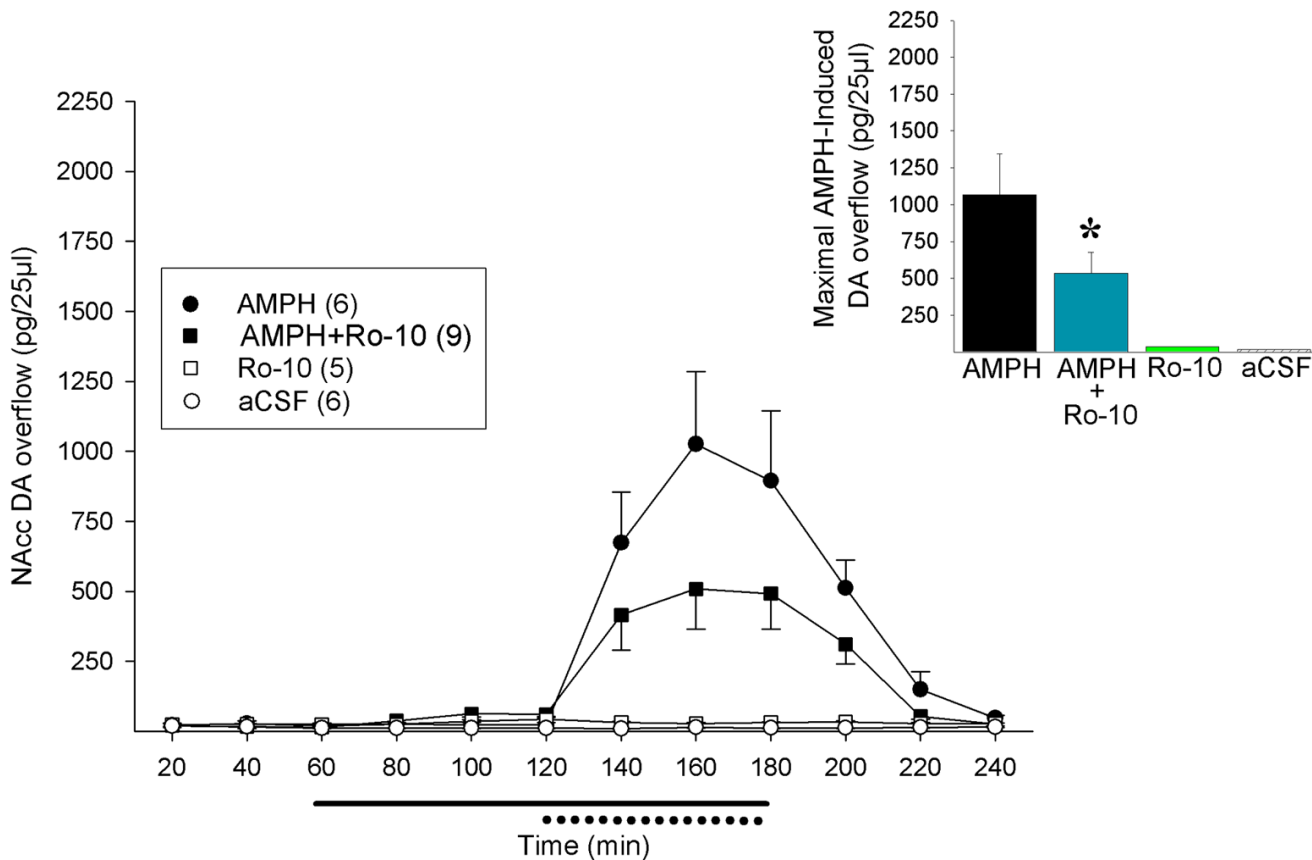


Figure 3. The PKC inhibitor Ro31-8220 attenuates the ability of AMPH to increase extracellular DA in the NAcc shell

Data are illustrated as described in Figure 2. *, $p < 0.05$, AMPH vs. AMPH + Ro31-8220.

Numbers in the legend indicate experiments/group.

Table 1

Effects of Ro31-8220 alone on extracellular levels of DA in the NAcc core and shell.

	aCSF	Ro31-8220 (10 μ M)	Ro31-8220 (100 μ M)
NAcc Core	37.2 \pm 8.3 (11)	40.7 \pm 9.4 (12)	162.1 \pm 53.8 (13) **
NAcc Shell	21.5 \pm 4.9 (12)	58.8 \pm 7.5 (14)	243.9 \pm 85.6 (12) **

Data are shown as group mean (\pm SEM) maximal DA overflow (pg/25 μ l) observed after introduction of Ro31-8220 (0, 10 or 100 μ M) into the aCSF in the second hour of testing. Maximal overflow for each animal was taken as the highest DA peak obtained during this period. One-way ANOVA detected significant effects of groups in the NAcc core ($F_{2,33}=6.44$, $p<0.01$) and shell ($F_{2,35}=10.53$, $p<0.001$). Post-hoc LSD tests revealed that the 100 μ M concentration significantly increased extracellular DA levels relative to the two other conditions. These did not differ significantly from each other. No group differences were detected in basal DA levels in the first hour of testing prior to introduction of Ro31-8220.

** $p<0.01$, Ro-100 significantly greater than two other groups. Numbers in parentheses indicate experiments/group.